Molecular Genetics and Metabolism 103 (2011) 367–377

Contents lists available at ScienceDirect

Molecular Genetics and Metabolism

journal homepage: www.elsevier.com/locate/ymgme

CNS-targeted AAV5 gene transfer results in global dispersal of vector and prevention of morphological and function deterioration in CNS of globoid cell leukodystrophy mouse model

Dar-Shong Lin [a,b,c,g,*], Chung-Der Hsiao [h], Ian Liau [i], Shuan-Pei Lin [a,c], Ming-Fu Chiang [d,e], Chih-Kuang Chuang [b,g], Tuen-Jen Wang [f], Tsu-Yen Wu [b], Yuan-Ren Jian [b], Sung-Fa Huang [f], Hsuan-Liang Liu [g,*]

[a] Department of Pediatrics, Mackay Memorial Hospital, Taipei, Taiwan
[b] Department of Medical Research, Mackay Memorial Hospital, Taipei, Taiwan
[c] Mackay Medicine, Nursing and Management College, Taipei, Taiwan
[d] Department of Neurosurgery, Mackay Memorial Hospital, Taipei, Taiwan
[e] Institute of Injury Prevention and Control, Taipei Medical University, Taipei, Taiwan
[f] Department of Laboratory Medicine, Mackay Memorial Hospital, Taipei, Taiwan
[g] Department of Chemical Engineering and Biotechnology, National Taipei University of Technology, Taipei, Taiwan
[h] Department of Bioscience Technology, Chung Yuan Christian University, Chung Li, Taiwan
[i] Department of Applied Chemistry, National Chiao Tung University, Hsinchu, Taiwan

ARTICLE INFO

Article history:
Received 4 May 2011
Accepted 6 May 2011
Available online 12 May 2011

Keywords:
Globoid cell leukodystrophy
Lysosomal storage disease
Adeno-associated virus
Purkinje cells

ABSTRACT

Globoid cell leukodystrophy (GLD) is a devastating lysosomal storage disease caused by deficiency of the enzyme galactocerebrosidase (GALC). Currently, there is no definite cure for GLD. Several attempts with CNS-directed gene therapy in twitcher mice (a murine model of GLD) demonstrated restricted expression of GALC activity in CNS and failure of therapeutic efficacy in cerebellum and spinal cord, resulting in various degrees of correction of biochemical, pathological and clinical phenotype. More recently, twitcher mice receiving a combination of hematopoietic and viral vector gene transfer therapies were not protected from neurodegeneration and axonopathy in both cerebellum and spinal cord. This evidence indicates the requirement of sufficient and widespread GALC expression in CNS and rescue of cerebellum and spinal cord in the therapeutic intervention of murine model of GLD. In this study, we have optimized intracranial delivery of AAV2/5-GALC to the neocortex, hippocampus and cerebellum, instead of the thalamus as was previously conducted, of twitcher mice. The CNS-targeted AAV2/5 gene transfer effectively dispersed GALC transgene along the neuraxis of CNS as far as the lumbar spinal cord, and reduced the accumulation of psychosine in the CNS of twitcher mice. Most importantly, the treated twitcher mice were protected from loss of oligodendrocytes and Purkinje cells, axonopathy and marked gliosis, and had significantly improved neuromotor function and prolonged lifespan. These preclinical findings with our approach are encouraging, although a more robust response in the spinal cord would be desirable. Collectively, the information in this study validates the efficacy of this gene delivery approach to correct enzymatic deficiency, psychosine accumulation and neuropathy in CNS of GLD. Combining cell therapy such as bone marrow transplantation with treatment with the aim of reducing inflammation, replacing dead or dying oligodendrocytes and targeting PNS may provide a synergistic and more complete correction of this disease.

1. Introduction

Globoid cell leukodystrophy (GLD; OMIM# 245200) or Krabbe disease is a devastating lysosomal storage disease caused by deficiency of the enzyme galactocerebrosidase (GALC; EC 3.2.1.46) [1,2]. The GALC enzyme is responsible for the degradation of galactocerebroside, a major glycolipid of central and peripheral myelin. A failure to adequately degrade galactocerebroside results in the accumulation of galactosphingosine (psychosine) which in turn leads to global demyelination in the central (CNS) and peripheral nervous systems (PNS), rapidly progressing degeneration, and early death. Affected infants with GLD manifest as early as 3–6 months of age with irritability, dysphagia, spasticity, cognitive and sensory deterioration, and seizures, and usually die by two years of age [2]. Twitcher mouse is an authentic murine model of GLD caused by

Abbreviations: GLD, globoid cell leukodystrophy; GALC, galactocerebrosidase; AAV, adeno-associated virus; CNS, central nervous system; PNS, peripheral nervous system; LSD, lysosomal storage disease; LINCL, late infantile neuronal lipofuscinosis.

* Corresponding authors at: Department of Pediatrics, Mackay Memorial Hospital, 92, Section 2, Chung-Shan North Road, Taipei 10449, Taiwan. Fax: +886 2 2809 4679.
E-mail addresses: dslin@ms1.mmh.org.tw (D.-S. Lin), contax@ms1.mmh.org.tw (H.-L. Liu).

1096-7192/$ – see front matter © 2011 Elsevier Inc. All rights reserved.
doi:10.1016/j.ymgme.2011.05.005

mutations in the *GALC* gene, lacks GALC activity, exhibits psychosine accumulation and recapitulates faithfully the clinical features and neuropathologic findings of human GLD. Therefore, it is widely used to investigate both the disease pathogenesis and the efficacy of novel therapies [3].

To date, there is no definite cure for the infantile form of GLD because of the rapid deterioration of neurological functions. Although both early bone marrow transplant (BMT) and umbilical cord stem cell transplantation have been shown to be beneficial in treating twitcher mice and presymptomatic GLD infants, respectively, the long-term outcomes of these approaches remain questioned in that treated twitcher animals eventually succumbed to the disease and patient recipients still exhibited progressive neurologic deterioration [4,5]. The practical therapeutic values of the transplantation of stem cells for the rapidly progressive form of GLD may be limited by the long lag time required to replace the defective host microglia with donor microglia expressing normal GALC enzyme in the CNS. Therefore, an alternative approach is urgently needed. Gene therapy has been shown to have great potential as the therapeutic approach for lysosomal storage disease (LSD), because of the broad tropism, rapid uptake and expression, and long-term transduction of affected cells [6]. Several preclinical CNS-directed gene therapy studies in twitcher mice have demonstrated various degrees of correction of biochemical, pathological and clinical phenotype [7–10].

Given the global involvement of CNS and rapidity of neurological deterioration in GLD, it is crucial to design therapeutic strategies that distribute therapeutics rapidly throughout the CNS before the disease progresses. Earlier, we showed that AAV2/5-GALC injection into neocortex, thalamus and hippocampus indeed expressed transgenic GALC throughout multiple brain regions and slowed down the decline of neurological functions [9]. Moreover, we also showed that the therapeutic efficacy of intracerebral delivery of AAV2/5-GALC in twitcher mice could be further enhanced with BMT, resulting in supraphysiological levels of GALC activity in the brain, prolonged lifespan up to 150 days, and significantly improvement of neurobehavioral performance [11]. However, the twitcher mice receiving a combination of CNS-directed gene therapy and BMT eventually died of neurological deterioration. The failure of widespread transgene expression, and lack of or low GALC expression in several important CNS regions such as the cerebellum, brain stem and spinal cord may at least partially account for the eventual failure of this intracerebral-based AAV approach [11]. More recently, Galbiati et al. observed similar results in which twitcher mice that had received a combination of hematopoietic and lentiviral gene transfer therapies, leading to a recovery of ~30% of normal GALC activity, were not protected from neurodegeneration and axonopathy in both the cerebellum and spinal cord [12]. Consistently, restricted GALC activity in CNS and failure of therapeutic efficacy in the cerebellum and spinal cord were also observed in a number of studies using viral vectors delivered by strategies utilizing different approaches such as intraventriclar, intracerebral and external capsule injection in twitcher mice [7,8,10]. Collectively, such evidence indicates the requirement of sufficient and widespread GALC expression in CNS and rescue of cerebellum and spinal cord in the therapeutic intervention of murine model of GLD.

In this study, we have optimized intracranial delivery of AAV vector to assess the therapeutic potential for treating the neurological disease in murine model of GLD. AAV2/5-GALC was injected into the neocortex, hippocampus and cerebellum, instead of thalamus as previously conducted [9,11], of twitcher mice. Evidence regards to cerebellum-targeted gene therapy in several animal models has shown efficacy in distributing vectors/proteins and rescuing of neuropathology in the cerebellum, midbrain, brain stem and spinal cord based on the mechanism of axonal transportation. We demonstrated that a gene therapy targeting neocortex, hippocampus and cerebellum indeed achieved a broad dispersal of viral vectors throughout the CNS, including the brain and spinal cord, functional recovery of GALC activity, and diminished the accumulation of psychosine in the brain. The AAV2/5-GALC treated twitcher mice exhibited a significant restoration of loss of oligodendrocytes and Purkinje cells, amelioration of marked gliosis in the brain, improvement of motor functions and extended lifespan. These results indicate that a CNS-targeted gene therapy may serve as the basis to develop more efficacious treatment for the murine model of GLD.

2. Materials and methods

2.1. Animal procedures

Heterozygous (*twi*/+) twitcher mice with a congenic C57Bl/6 background were originally obtained from The Jackson Laboratories and maintained in the animal research facility of our institution under standard housing conditions in a pathogen-free environment. Homozygous (*twi*/*twi*) twitcher mice and normal (+/+) controls were obtained by strict inbred matings of heterozygous animals and the genotyping of newborn mice was determined by PCR specific for the Twitcher mutation [13]. Mice surviving up to an age of 21 days were enrolled in this study. All animal procedures were approved by, and carried out in accordance with the regulations established by our institution.

2.2. Body weight assessment and survivability

For an objective measure of development and disease progression, mice were weighed weekly throughout their lives starting from the seventh postnatal day until death or if they became moribund, at which time they were euthanized after general anesthesia for humane reasons. To determine survivability, mice were maintained humanely in accordance to the norms of ethical laboratory animal care with free access to food and water. The mice were euthanized humanely when they reached a moribund state.

On postnatal day three, the twitcher mice received six intracranial injections of AAV encoding GALC. The animals were injected at three sites per hemisphere; the sites of the injections included the cerebellar vermis (3.5 mm caudal and 2 mm lateral from the lambda and 1.5 mm deep), cortex (2 mm caudal and 2 mm lateral from the bregma and 2 mm deep), and the hippocampus (3.5 mm caudal and 2 mm lateral from the bregma and 1.5 mm deep). The animals received 2.4×10^9 particles of AAV2/5 at each injection site in a volume of 2 μl using a 30-gauge needle attached to a 5-μl Hamilton syringe (Hamilton Company, Reno, NV). Untreated twitcher and normal control mice were included as controls in this study.

2.3. Recombinant AAV2/5 vector

The AAV2/5 vector used in this study has been previously described. Briefly, it contained serotype-2 inverted terminal repeats and murine GALC cDNA under the control of CMV enhancer and chicken-β-actin promoter (CBA) [11]. The detailed description of the production of AAV2/5 vectors was reported previously [11]. Briefly, the vector was produced by co-transfection of HEK293 cells with vector plasmid and helper plasmid harboring the adenoviral helper sequences as well as the AAV2 Rep and Cap5 genes. The AAV2/5 vector was purified by cesium chloride gradient centrifugation followed by extensive desalination via dialysis in Ca^{2+}/Mg^{2+}-containing Dulbecco's Phosphate Buffered Saline buffer. DNase-resistant viral genome copies were determined by Dot blot hybridization and compared to known quantities of vector plasmid.

2.4. Tissue harvesting, processing, GALC activity and psychosine

Mice were euthanized under anesthesia with avertin. The entire brain and spinal cord of each animal were immediately removed, snap frozen with liquid nitrogen and stored at −80 °C prior to biochemical analysis. Alternatively, mice were transcardially perfused with 4% paraformaldehyde (PFA). The entire brain and spinal cord of each animal were post-fixed in the same fixative overnight at 4 °C, cryoprotected in 30% sucrose, and then quickly frozen in OCT compound (TissueTek, Sakura Finetek, Torrance, CA). Blocks were sliced on a cryostat at 8-μm thickness, and stored at −80 °C prior to immunohistochemistry and regular histology.

To determine the distribution of GALC activity in the CNS after AAV2/5 injection, hemisphere brain tissues were dissected into six (S1–S6) sections and spinal cord tissues into cervical (S7), thoracic (S8) and lumbar (S9) sections (Fig. 2). Frozen tissues were thawed on ice and were homogenized in deionized water as previously described [9]. The protein concentration was determined in diluted samples of hemogenates with a commercially available Coomassie dye-binding assay (Bio-Rad, Hercules, CA) using bovine serum albumin as standard. GALC activity was determined with [^{3}H]galactosylceramide substrate according to previously published methods [14].

Psychosine levels were determined in the same homogenates used for measurement of GALC activity using the LC/MS method prescribed previously [15]. Briefly, homogenates with internal standard lactosylsphingosine were added to 1% formic acid/methanol solution, then allowed to stand for 1 h at room temperature, followed by centrifugation at 1800 *g* for 15 min at 4 °C. The supernatant was collected, blown to dryness, and resuspended in 0.1% formic acid/78% methanol solution, followed by sonication for 15 min and centrifugation at 1800 *g* for 15 min. The supernatant was filtered and analyzed on an API 365 LC/MS (Applied Biosystems, Forster City, CA, USA).

2.5. Histochemical localization of GALC activity

The modified histochemical staining method for *in situ* localization of GALC activity was performed as previously described [16]. Briefly, 8 μm-thick cryosections were equilibrated in citrate/phosphate buffer (pH. 4.2, C/P buffer), followed by incubation with taurodeoxycholic/oleic acids in C/P buffer, then stained with X-Gal solution containing taurodeoxycholic/oleic acids in C/P buffer. Sections were counterstained with nuclear fast red (Sigma).

2.6. Immunohistochemistry

Cryosections were fixed with 4% PFA for 20 min, quenched with 3% H_2O_2 in methanol for 5 min, and permeabilized with 0.5% Triton X-100 for 10 min. After being blocked in 2.5% goat serum/0.25% Triton X-100 in phosphate buffered saline (PBS) for 2 h at room temperature, sections were incubated with primary antibodies over night at room temperature. Astrocytes were labeled with mice anti-glial fibrillary acid protein (GFAP; 1:500, Vector Laboratory), and microglias were labeled with mice anti-ionized calcium-binding adapter molecule-1 (Iba1; 1:200, WAKO). Antibodies were detected using goat anti-mice HRP polymer (EnVision, PRESS, DAKO). Sections were visualized by adding diaminobenzidine substrate (DAB+, DAKO) and counter-stained with hematoxylin. For immunofluorescence, Purkinje cells, oligodendrocytes, myelin and axonal degeneration were labeled with mouse anti-calbindin (1:200, Sigma), mouse anti-2′,3′-Cyclic nucleotide 3′-phosphodiesterase (CNPase; 1:100, Chemicon), mouse anti-myelin basic protein (MBP; 1:100, Chemicon), and mouse anti-amyloid precursor protein (APP ; 1:200, Chemicon), respectively, and visualized with Alex Flour 488 goat anti-mice IgG (1:100, Molecular Probes). Nuclei were stained with DAPI.

2.7. Analysis of vector genome

Recombinant AAV vector expressing mouse GALC cDNA was detected in brain and spinal cord tissue by nested PCR as described previously [8]. Briefly, genomic DNA was extracted using the Qiagen DNAeasy Tissue Kit. Two hundred nanogram of DNA was used for PCRs. The vector genome was then amplified using specific primers for mouse GALC cDNA without amplifying the genomic GALC DNA [8]. All samples were analyzed in triplicate. A 283-bp PCR product was analyzed by electrophoresis in 3% gel. Glyceraldehyde-3-phosphate dehydrogenase (GAPDH) was amplified as an internal control. Viral copy number (VCN) were quantified by quantitative real-time (RT) PCR amplifying CBA promoter of the AAV2/5 in an ABI Prism 7700 Sequence detection system (Applied Biosystems, Darmstadt, Germany) by using SYBR green I as a double-strand DNA specific binding dye.

2.8. Behavioral phenotyping

Experimental and control mice were challenged repeatedly in a grip strength test to evaluate neuromuscular function. Animals were randomly labeled and tested every 7 days starting at 21 days of age. The experimenters were blinded with regards to the genotype and therapeutic regimen. Mice were held gently by the tail and lowered toward the grip strength meter (Columbus, OH) so that only the front paws were able to grip the T-bar. With the torso in a horizontal position the mice were pulled back steadily until the grip was released. The maximum force applied was recorded as the peak tension (gram). The highest value from the 3 consecutive trials was recorded as the forelimb grip strength for that animal.

2.9. Statistical analyses

All data are expressed as mean values ± 1 SEM. Comparisons of the life span between-group were performed using Kaplan–Meier analysis. For behavioral comparisons, between-group differences at each age were determined by two-way-ANOVA with the post hoc Bonferroni method. Differences were considered significant at $p<0.05$.

3. Results

3.1. GALC distribution

To analyze the distribution of transgenic GALC expression, 8 μm-thick cryosections of brain and spinal cord from treated and control mice were stained histochemically for GALC activity with X-gal after inhibiting endogenous β-galactosidase activity as previously described [16]. As expected, we detected intense GALC-positive signal in the CNS of AAV2/5-GALC-injected twitcher mice (Fig. 1), whereas the corresponding structures in untreated twitcher mice were stained negative, indicating that the staining detected was from the AAV2/5-transduced GALC protein. In more detailed analysis of the distribution pattern, the vector-encoded GALC enzyme was intensively stained within the thalamus and the entire cerebral cortex extending from the anterior area of the frontal lobe to the posterior area of the visual cortex. The cortical expression of GALC was mainly localized to the gray matter, with little GALC-positive staining seen in the corpus callosum and striatum. In addition, there was intense GALC-staining in the pyramidal neurons of the CA1, CA2 and CA3 regions of the hippocampus. Prominent enzymatic staining was also observed in the ependymal layers of the lateral ventricles, the third and the fourth ventricles, choroids plexus, and meningeal lining, indicative of partial vector leakage/reflux from the injection tract into the ventricles. In the cerebellum, GALC-staining was visible mainly in the Purkinje cell layer. In addition to GALC staining of individual neuronal bodies in the neocortex, thalamus, and hippocampus, there was also GALC staining

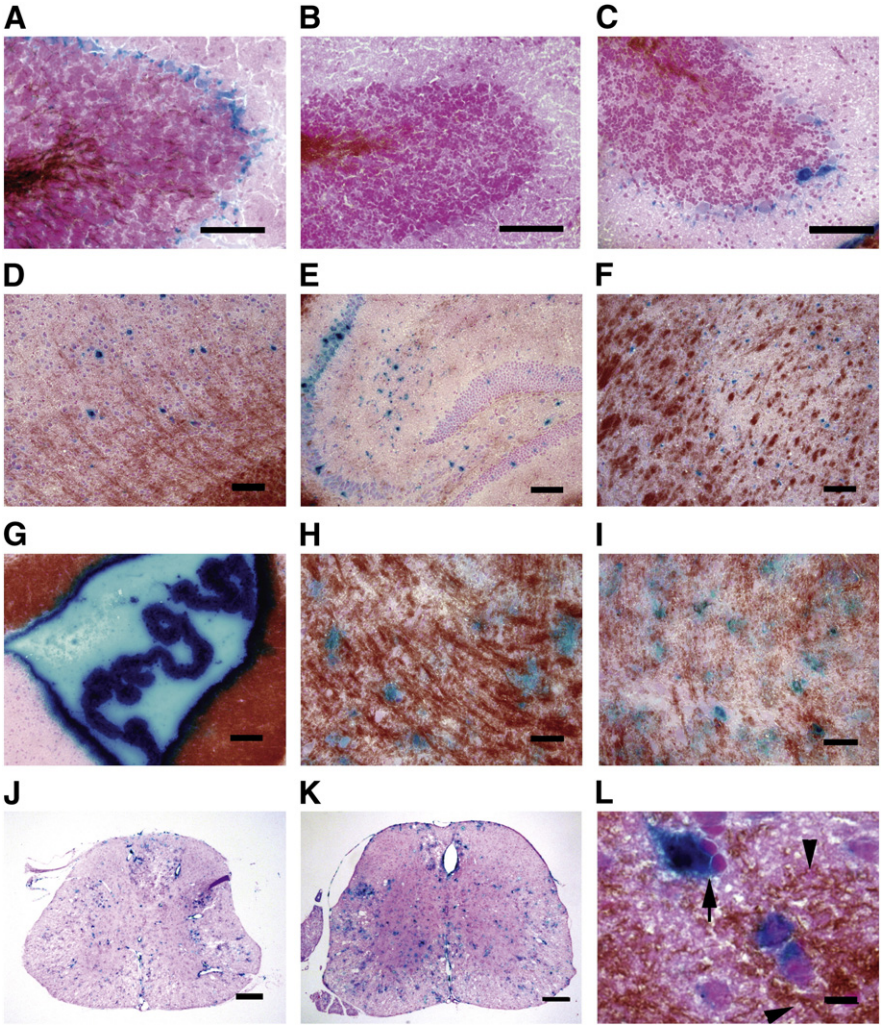

Fig. 1. Global distribution of GALC expression in CNS and spinal cord of twitcher mouse after AAV2/5 gene therapy. GALC activity in cryostat sagittal sections (8 μm) of brain from a 65-day-old wild-type mouse (A), 40-day-old untreated twitcher mouse (B) and 65-day-old AAV2/5-treated twitcher mouse (C–L) was shown as the blue staining using X-Gal histochemical detection and counter stained with nuclear fast red, where the white matter was immunostained brown using anti-CNPase antibodies. Cerebellum (A–C), cortex (D), hippocampus (E), thalamus (F), lateral ventricle (G), brain stem(H) , and the whole spinal cord (sagittal section of cervical spinal cord, I; transverse section of thoracic cord, J, and lumbar cord, K). At higher magnification (L), the GALC-positive cells demonstrated a neuronal morphology, and oligodendrocytes (brown; arrowhead) located proximally to GALC-positive neurons showed normal appearance. The GALC activity diffused from the intense stained GALC-positive neurons to surrounding cells (arrow) (L). (scale bars : A–C, 200 μm; D–I, 200 μm; J–K, 200 μm; L, 20 μm).

in the parenchyma of brain stem and spinal cord, indicative of transport from the injected sites. The whole spinal cord was examined histochemically. Many GALC-positive cells had the morphology of neuronal identity in the anterior and posterior horns of the gray matter along the entire length of spinal cord.

3.2. GALC level and psychosine accumulation

For biochemical analysis, a brain hemisphere and spinal cord of GALC-treated and control animals were dissected into 9 slabs (Fig. 2), homogenized, and further analyzed for GALC activity. GALC specific activities in the brain and spinal cord segment of untreated twitcher mice were barely detectable (0.03 ± 0.02 nmol/h/mg protein) (Fig. 2A), much lower than those in corresponding areas of wild-type mice (2.14 ± 0.69 nmol/h/mg protein). In contrast, GALC activity in the brain of AAV2/5-GALC-treated twitcher mice ($n = 6$, 57–64 days) was significantly elevated compared to that of untreated twitcher mice ($p < 0.001$), and the level of increase varied among various regions. For instance, GALC activity in regions corresponding to the injection sites S1, S3, and S6 exhibited an enzyme activity 3–5 fold higher than normal, and the three adjacent regions S2, S4, and S5 had an GALC activity 1.5–1.8 fold of normal (Fig. 2A). Interestingly, AAV2/5-GALC-treated twitcher mice (57–64 days) had modest increased levels of GALC activity in the spinal cord regions S7–S9 (0.155 ± 0.06 nmol/h/mg protein, $p < 0.05$), which was equivalent to 6% of wild type GALC activity. The AAV2/5-GALC-treated twitcher mice showed level of enzyme activity at 35 days similar to those measured at 57–64 days. Since there had been no direct injection into the spinal cord, the mild increase in spinal GALC activity indicated the transport of AAV2/5-GALC from the transduced cells in the injection sites along the whole spinal cord. PCR analysis of the brain slabs and spinal cord segments of treated twitcher mice confirmed the presence of the AAV2/5-GALC construct and further substantiated widespread distribution of viral vectors throughout the CNS and whole spinal cord (Fig. 2C). The level of transgene by PCR generally matched with the levels of GALC activity in the individual slabs. The validity of PCR results was supported by the absence of this product in untreated twitcher mice. The quantitative RT-PCR (Fig. 2D) further validates the wide distribution of vector along neuraxis of CNS. The sciatic nerves of AAV2/5-GALC-treated

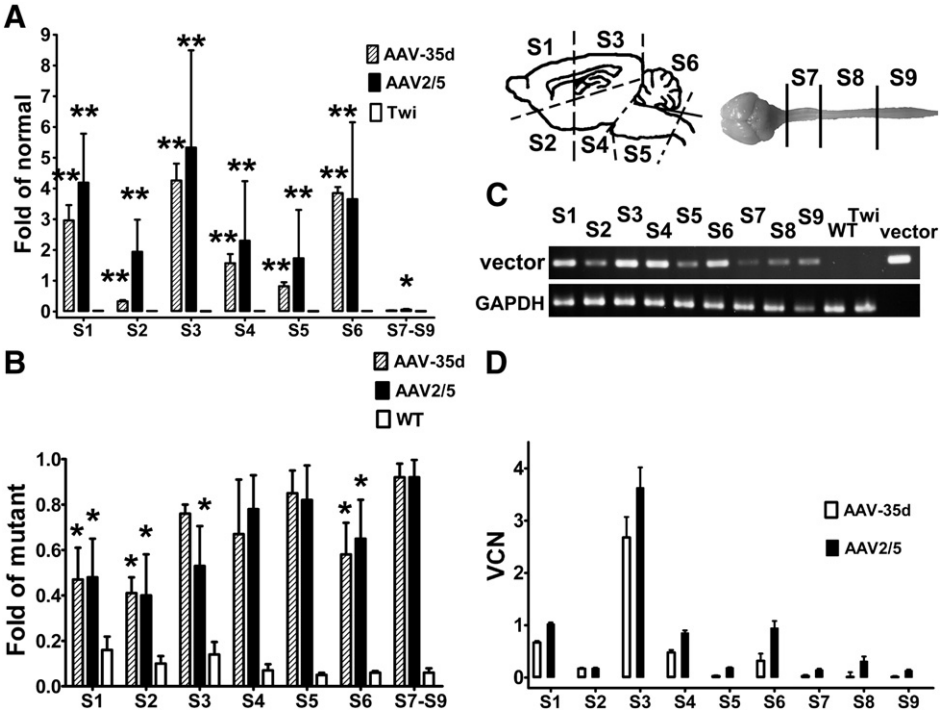

Fig. 2. Increase in GALC activity relative to normal and reduction of psychosine accumulation relative to mutant in various CNS regions of AAV2/5-treated Twitcher mice. GALC activity (A) and psychosine accumulation (B), expressed as a fold of normal and fold of mutant, respectively, were measured in the same homogenates of brains and spinal cords of AAV2/5-treated twitcher at 35 days (AAV-35 d, n = 3) and at 57–64 days (AAV2/5, n = 6), untreated twitcher (Twi, n = 6, 38 days) and wild-type mice (WT, n = 6, 56 days). AAV2/5 viral genome was identified by PCR (C) and quantitative RT-PCR (D) in the slabs of brain and spinal cord of treated twitcher mice. * Indicates significance of $p<0.05$ between AAV2/5-treated twitcher mice and untreated twitcher mice. ** Indicates significance of $p<0.001$ between AAV2/5-treated twitcher mice and untreated twitcher mice. The bars represent the mean ± 1 SEM.

twitcher mice showed barely detectable levels of enzyme activity, nondetectable viral vectors genome, and edematous neuropathy similar to those of untreated twitcher mice (data not shown).

The accumulation of psychosine, which correlated well with the neuropathology in GLD and twitcher mice [17,18], began as early as the embryonic stage, and was most abundant in the hindbrain, spinal cord and peripheral nerve. To determine if the increase in the GALC activity was physiologically relevant, we examined the levels of psychosine in the same slabs used for GALC activity assay. We expected the GALC activity supplied by the viral vector would catalyze the hydrolysis of psychosine. Consistent with our expectation, mass spectrometry quantification revealed that an increase in the GALC levels in the brain significantly decreased psychosine accumulation in the cortex (S1), hippocampus (S3) and cerebellum (S6) of AAV2/5-GALC-treated twitcher mice (n = 6, 57–64 days), compared to those in corresponding areas of untreated twitcher mice (Fig. 2B). However, psychosine level in brain of wild-type mice (0.247 ± 0.024 pmol/mg protein; $p<0.001$) remained significantly lower than that in untreated twitcher mice (3.43 ± 1.026 pmol/mg protein) and AAV2/5-GALC-treated twitcher mice (2.209 ± 1.148 pmol/mg protein; n = 6, 57–64 days). The AAV2/5-GALC-treated twitcher mice showed level of psychosine accumulation at 35 days similar to those measured at 57–64 days.

3.3. Reduced inflammatory markers in the brain

Inflammation in the CNS of twitcher mice progressed in an orderly fashion such that infiltration of astrocytes and macrophages was recognized first in the cerebellar white matter and the brain stem after postnatal day 20, then in cerebral white matter, and finally in cerebral and cerebellar gray matter after postnatal day 30 [19]. Our results were similar to previous studies in that activation of Iba-1-positive microglia was recognized remarkably throughout the white matter tracts of the cerebellum, cerebrum, and spinal cord in untreated twitcher mice (Fig. 3). Injections of AAV2/5-GALC dramatically reduced the number of microglia in the cerebrum and cerebellum to the level similar to that of wild-type mice. However, AAV2/5-GALC had little or no effect on Iba-1 staining in the spinal cord, albeit there was modest GALC activity.

Widespread astrocytosis, as assessed by immunostaining for glial fibrillary acidic protein (GFAP), was observed throughout the cerebral cortex, striatum, cerebellum and spinal cord of untreated twitcher mice when compared to wild-type mice (Fig. 3). Similar to the results obtained with Iba-1 staining, treatment with AAV2/5-GALC resulted in a global reduction of GFAP staining in the whole brain and cerebellum. However, twitcher mice receiving the AAV2/5-GALC treatment still had intense GFAP staining in the spinal cord.

3.4. CNS myelination histopathology

2′,3′-Cyclic nucleotide 3′-phosphodiesterase (CNPase) localized on cytoplasmic membrane of oligodendrocytes and Schwann cells plays an important role in the myelination process as well as in the maintenance of the myelin sheath. Demyelination has been reported as a major neuropathology in twitcher mice, which was causally linked to the decrease in CNPase activity of the brain cortex, brain stem and spinal cord of the twitcher mice [20], therefore, the alteration in the status of oligodendrocytes could be evaluated by immunofluorescent labeling using anti-CNPase antibodies. As revealed in Fig. 4, severe loss of the CNPase signals occurred in neocortex, cerebellum and spinal cord, but myelination was remarkably preserved in neocortex and cerebellum in AAV2/5-treated twitcher mice compared with non-treated animals. As a matter of fact, both the intensity and architecture of the CNPase signals in treated twitcher mice approached those of the wild type mice. CNPase-labeled axons in neocortex were evenly spaced and properly aligned in parallel. In the cerebellum, more myelinated axons were observed in the granular layer and expanded into the Purkinje cell

layer in treated twitcher mice, a staining patter similar to that found in wild-type mice. The prevention of demyelination in brain by AAV2/5 treatment was further elucidated by the intense MBP signals in striatum (Fig. 4).

3.5. Calbindin-positive cells in the Purkinje cell layer

Calbindin is a widely accepted Purkinje cell marker. By calbindin immunohistochemical staining, we found a mark reduction in the overall number of Purkinje cells and accompanied cerebellar astrogliosis in the twitcher mice at the moribund stage. Strikingly, in the AAV2/5-GALC treated twitcher mice, the Purkinje neurons of the cerebellum were remarkably preserved compared to wild type mice (Fig. 5). No obvious reduction in the number of Purkinje cells was appreciated, and minimal astrogliosis was observed only in the late-stage of GLD disease (Fig. 3), similar to that found in wild-type mice. Interestingly, the calbindin-positive Purkinje cells had intense GALC activity. Our results indicate that AAV2/5-mediated GALC expression in the cerebellum of the twitcher mice significantly improved Purkinje cell survival and attenuated astrogliosis in both the granule and Purkinje cell layers.

3.6. Axonal degeneration in twitcher mice

A recent study of twitcher mice receiving bone marrow cells transduced with a lentivirus encoding the human GALC gene showed that axonal degeneration was observed in those long-term survival twitcher mice [12]. To investigate the axonal injury, we further examined the expression of amyloid precursor protein (APP), a marker for axonal degeneration, by immunofluorescent labeling on the sagittal section of the CNS. Upon examination, we found very strong immunoreactivity for APP in the white matter of cerebellum and brain stem of untreated twitcher mice (Fig. 5), consistent with reported active axonal degeneration. In sharp contrast, the white matter of the corresponding regions from treated twitcher mice showed no APP accumulation similar to that of wild-type mice. Our data indicated a complete prevention of axonal degeneration by AAV2/5-GALC gene therapy.

3.7. Rescue of neuromuscular function, improve survival, and maintenance of body weight

To investigate the ability to restore neuromuscular function, grip test was used to assess the neuromuscular strength of the forelimbs of the experimental and control mice (Fig. 6A). Similar to previous reports, the untreated twitcher mice showed significantly weaker neuromuscular function which reached plateau from day 21 to day 35 and declined precipitously at 35 days of age. Interestingly, the gain of grip strength in AAV2/5-GALC-treated twitcher mice increased steadily up until 35 days of age, then declined slowly. The effect of GALC expression on the rescue of neurons and its translation into neuromuscular function was significantly evident in those AAV2/5-treated twitcher mice, compared to those untreated twitcher mice ($p<0.05$). Our results demonstrated a clear therapeutic benefit which extended down to the motor neurons of the spinal cord.

Mice were weighed weekly to evaluate overall fitness (Fig. 6B), and their survival were plotted on a Kaplan–Meier curve (Fig. 6C). Untreated twitcher mice showed a lag in weight gain in the early stage of illness, and then a precipitous weight lost in the later stages of illness. In contrast, weight loss in the twitcher mice after AAV2/5-GALC treatment was markedly delayed ($p<0.05$), reflecting maintenance of well-being, foraging, and feeding activity. Longevity studies were carried out to determine the therapeutic impacts of AAV2/5-GALC CNS gene delivery in twitcher mice. The mean lifespan of AAV2/5-GALC-treated twitcher mice was significantly increased to 62 ± 3 days (range 56–66 days, median = 63 days, $n=15$) ($p<0.001$), compared to the untreated twitcher mice (40 ± 2 days, median = 40 days, $n=15$). The delayed onset of degenerative symptoms, improvement of neuromuscular function and prolonged lifespan in the AAV2/5-GALC-treated twitcher mice suggested the successful delivery of the therapeutic vectors to the CNS using axonal transportation after intracranial injection.

4. Discussion

In this study, our results indicate a global GALC protein expression throughout the neuraxis, from the cerebral cortex to the whole spinal cord, by direct AAV2/5-GALC injection into the brain and cerebellum of neonatal twitcher mice. Interestingly, the GALC activity correlated with the presence of the vector genome near the injection sites, and also in regions distant from the injection sites, indicating a widespread transduction in the CNS resulting from the dispersal of AAV2/5-GALC vector. The presence of GALC activity and vector genome in regions remote from the injection sites may be explained by four possible mechanisms: (a) secreted enzyme from transduced cells in regions surrounding the injection site can be endocytosed and targeted to lysosome by cells in remote regions; (b) therapeutics may be transported axonally both antegrade and retrograde following direct intracranial delivery of a transgenic vector; (c) immaturities of neonatal brain; and (d) distribution through CSF flow.

4.1. Axonal transport of vector

Several therapeutic approaches by transducing selected regions possessing divergent axonal connection with transportable vector have shown promising results for the treatment of the CNS component of LSDs [21–24]. In this study, we included the intracerebellar injection based on its neuroanatomical connections with brain stem, mid brain, and spinal cord [23–25], together with administration of vectors into the hippocampus (to deliver vector and enzyme over ipsilateral and contralateral hippocampi along the anterograde and retrograde axonal pathway) [26], and into the sensory cortex (to distribute vectors into other cortex and subcortical gray matter like thalamus and basal ganglia) [27]. Consistent with previous studies [9,11,24], our AAV2/5-GALC vectors mainly transduced neurons and resulted in supraphysiological activity of galactocerebrosidase for functional restoration. Strikingly, very high levels of GALC were identified not only in regions surrounding the injection sites, but also in regions remote from the injections. Neuroanatomical mapping of GALC staining over the CNS and spinal cord was consistent with the pattern of distribution through major neuronal circuitry in the CNS [28,29], suggesting that the widespread dispersal of AAV2/5 was mediated by axonal transportation. Our findings were consistent with previous studies pertaining to axonal transportation of vectors in CNS after targeting brain regions with divergent axonal connections [23,26,27] . Additionally, polymerase chain reaction analysis of the vector genome further confirmed the dispersal of the vector from the injection sites rather than distribution of GALC proteins. It is speculated that the widespread of vector may be contributed to the CSF flow since there were intense GALC-positive stained ependymal cells and choroid plexus. In our studies, the molecular and enzymatic analysis together with the lack of non-preferential distribution of GALC expression throughout CNS

Fig. 3. Decrease in the numbers of macrophages/microglias and astrocytes by AAV2/5 treatment. The astrocytes (A–D) and macrophages/microglias (E–H) in brains from a 65-day-old wild-type mouse (WT), 40-day-old untreated twitcher mouse (Twi) and 65-day-old AAV2/5-treated twitcher mouse (AAV2/5) were detected by immunohistochemical methods using GFAP (A–D) and Iba-1 (E–H), respectively. Cortex (A, E), hippocampus (B, F), cerebellum (C, G), and spinal cord (D, H). (scale bars: 200 μm).

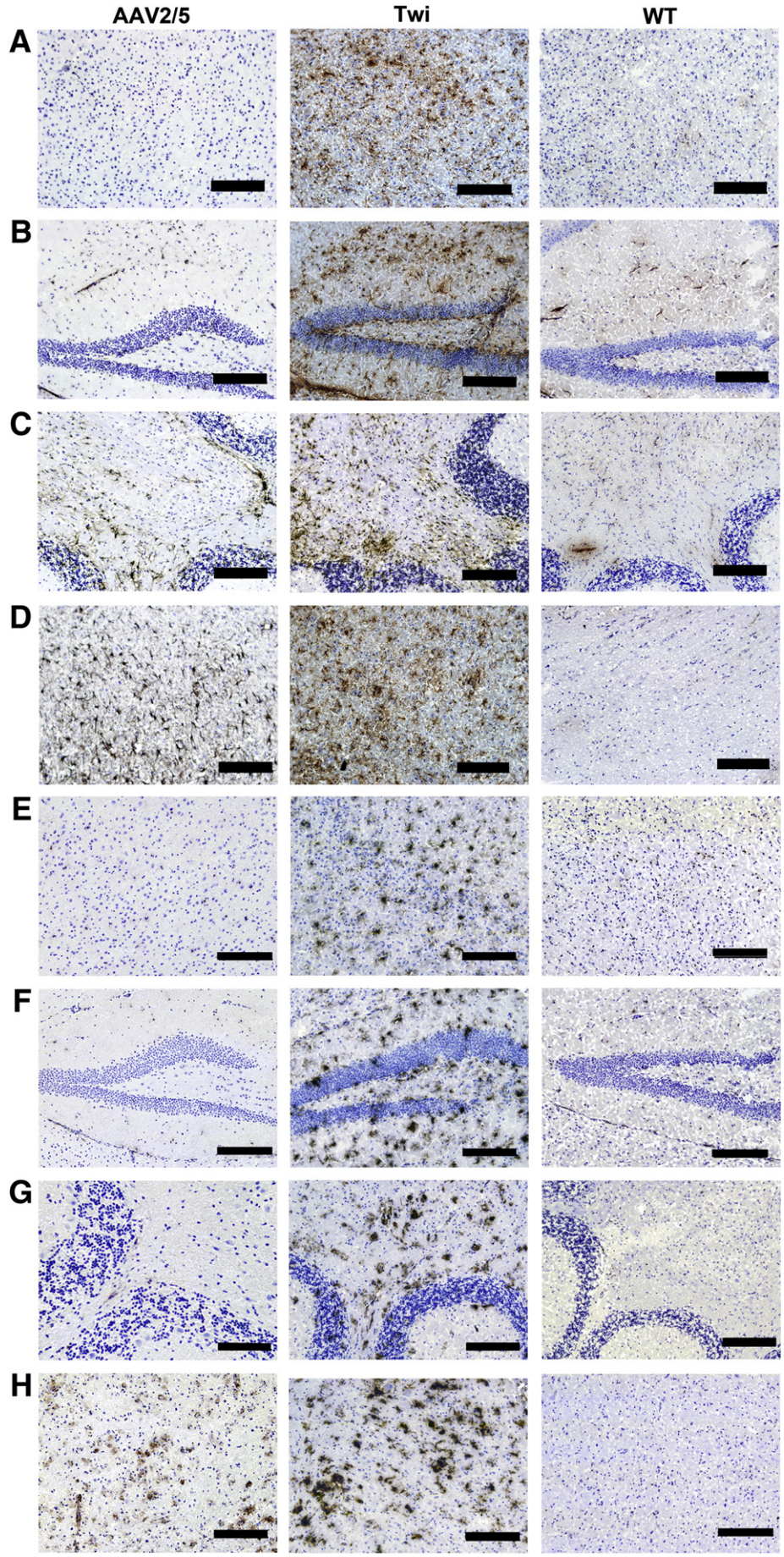
AAV2/5
Twi
WT
A
B
C
D
E
F
G
H

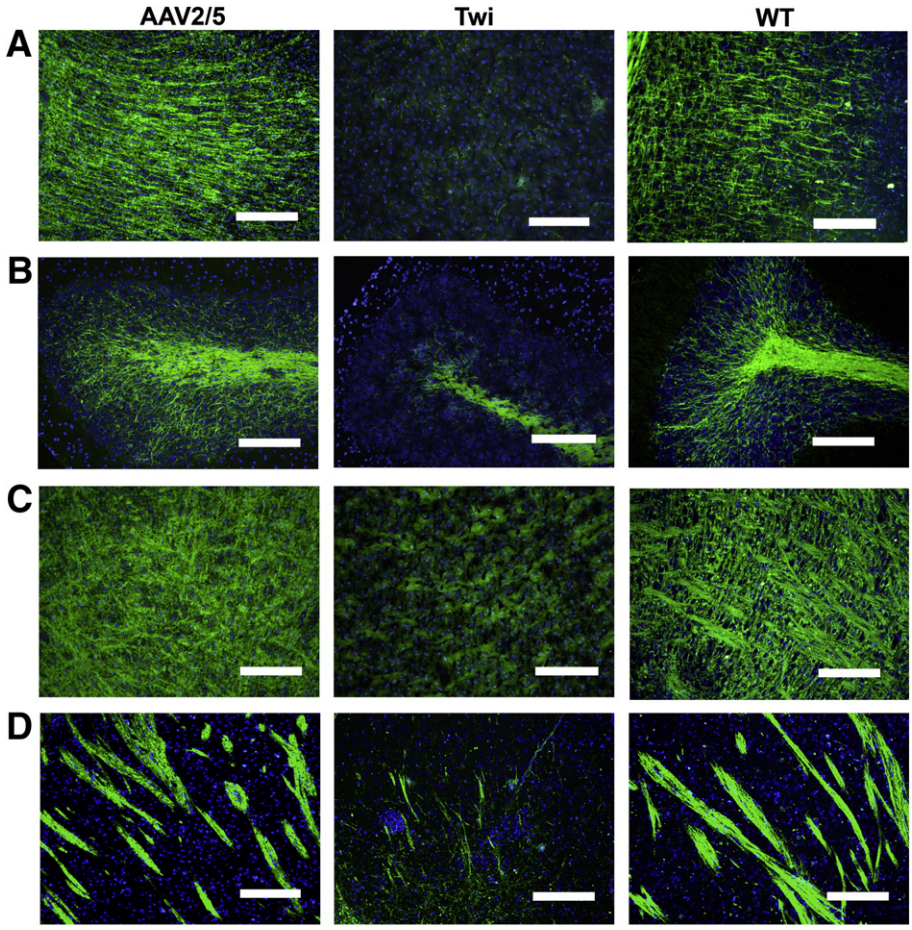

Fig. 4. The loss of oligodendrocytes was prevented by AAV2/5 treatment. Shown were sagittal brain sections from 65-day-old wild-type (WT), 42-day-old twitcher (Twi) and 65-day-old AAV2/5-GALC-treated (AAV2/5) twitcher mouse immunostained with anti-CNPase (green; A–C), and anti-MBP (green; D), respectively, and nuclear counterstained with DAPI (blue). Cortex (A), cerebellum (B), spinal cord (C), and striatum (D). (scale bars: 200 μm).

indicated that the mechanism of axonal transport prevails over CSF flow in ensuring widespread vector distribution in CNS.

4.2. Benefit of neonatal treatment

The lack of maturation of the brain in neonatal twitcher mice also raises concern in regard to AAV vector distribution. Therefore, another experiment using the same strategy of intracranial administration of AAV2/5-GALC at 10 days was performed, which showed a moderate distribution of GALC expression recapitalizing the pattern of axonal transportation in CNS as that treated at neonates and had no impact on lifespan (data not shown). This result was consistent with previous studies in an animal model of late infantile neuronal ceroid lipofuscinosis (LINCL) [30], and implied that the wide distribution of vector by our optimized therapeutic approach in neonatal twitcher mice may arise from a combination of factors rather than just axonal transportation of vector alone. With regards to endothelial cell permeability and maturity in newborn mice, earlier administration of intracranial gene therapy leads to a higher density and more widespread distribution of vectors within the CNS. The value of the neonatal window for treatment has been previously shown in several studies in models of LSD [7,31,32]. These reports, along with the results described in this paper, indicate that the more efficient transduction of the deeper neuronal structure is responsible for the benefits of neonatal gene therapy [30,32]. Moreover, a broader diffusion of vector particles from the injection sites, either in the gray matter or along the white matter tracts, has been described following injection of several AAV serotypes in the brain parenchyma [22,26,33]. Thus, the relative higher density of vector particle to brain volume, reduced barriers to diffusion of vectors in the much smaller and still developing neonatal brain may facilitate widespread distribution of delivered vector following intracranial-mediated gene therapy at neonates [30,32]. It seems likely that these factors coupled with axonal transportation could account for the widespread distribution of vectors and GALC activity observed in this study.

4.3. Protection from the loss of Purkinje cells

Previous studies in murine models of lysosomal storage disease have demonstrated that bone marrow-derived stem cells can effectively prevent the loss of Purkinje cells and alleviate inflammation via cell fusion after transplantation [34]. However, the neuropathologic changes of the cerebellum in twitcher mice remain vulnerable after BMT [9,11]. Interestingly, the results from our present study demonstrated rescue of Purkinje cells and amelioration of neuropathology in the cerebellum of AAV2/5-GALC-treated twitcher mice. This observation is consistent with a previous study in a mouse model of spinocerebellar ataxia in that a limited number of rescued Purkinje cells could substantially compensate for the cerebellar function and maintain the correct polarity and cytoskeletal arrangement of neuronal cells in the cerebellum [35]. Moreover, our results support the findings of Sevin et al. in that preserved Purkinje cells contribute to the prevention of neural degeneration, maintenance of the dendritic architectures and amelioration of inflammation

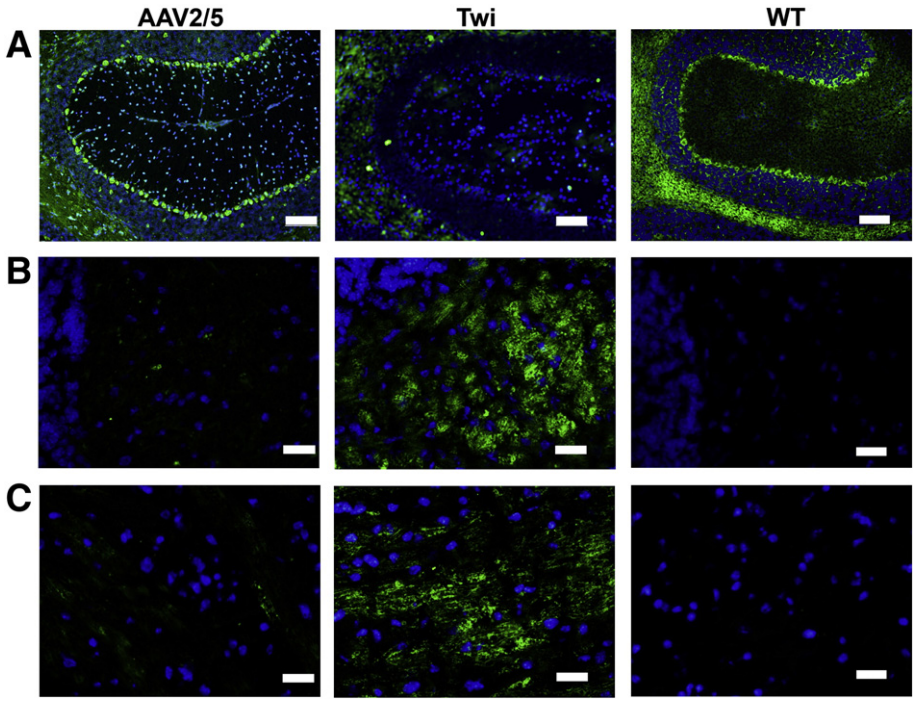

Fig. 5. Purkinje cells loss and axonal degeneration in twitcher mice were prevented by AAV2/5 injection. Brain sagittal cryosections from 65-day-old wild-type (WT), 42-day-old twitcher (Twi) and 65-day-old AAV2/5-GALC-treated (AAV2/5) twitcher mouse were immunostained with anti-calbindin (green; A, cerebellum) and anti-APP (green; B, cerebellum; C, brain stem), respectively, and nuclear counterstained with DAPI (blue). (scale bars: A, 100 μm; B–C, 50 μm).

in the cerebrum of metachromatic leukodystrophy mice [36], given the tropic and molecular support involving cerebellar synaptic interconnection. Overall, we showed that AAV2/5 vectors are capable of mediating effective transduction of Purkinje cells when introduced into the cerebellum, which is a much more efficient and effective means of delivering therapy to the whole cerebellum.

4.4. Prevention of loss of oligodendrocytes and axonopathy by cross-correction

In both human patients and murine model of GLD axonal degeneration develops contemporaneously with demyelination neuropathology. Axonal neuropathy remains vulnerable in twitcher mice receiving bone marrow transplantation alone or in combination with gene therapy [12], given the reduced myelin profiles in remyelinated axons and the slow recovery of corrective GALC enzyme activity in the CNS after treatment. Interestingly, our results showed that integrity of myelination and axons were preserved in the brains of twitcher mice after intracranial AAV2/5-mediated gene therapy. This therapeutic efficacy is likely contributed to the rapid expression and broad wide distribution of corrective enzyme along the neuraxis after the intracranial delivery of AAV2/5-GALC vector. By combination of X-gal staining and anti-CNPase immunostaining, oligodendrocytes surrounding GALC-positive neurons showed normal morphology in brains of AAV2/5-treated twitcher mice. Although oligodendrocytes are not the prime targets of AAV vector, our findings provide additional evidence consistent with previous studies that correction of the oligodendrocyte morphology can be attributed to uptake of GALC activity from neighboring GALC-transduced neurons [8,37,38]. The existence of these evidences for cross-correction of GALC-deficiency oligodendrocytes underlies the rationale that not all cells in the CNS have to be genetically modified to achieve therapeutic efficacy.

4.5. Insufficient rescue of spinal cord and optimal strategies in future

Although our approach resulted in the global distribution of injected vectors in the CNS, the restoration of GALC activity in spinal cords (6% of normal levels) was relatively weak compared to the supraphysiological GALC activity induced in brains (1.5–3 fold of normal). The neuropathology and accumulation of psychosine in spinal cords of AAV2/5-treated twitcher mice were not rescued by this low level of GALC activity, though enzyme activity representing as little as 1–5% of normal levels in the CNS is considered sufficient to promote neuropathology and rescue phenotype in murine models of LSD [39]. Rather, it is assumed that requirements of up to 50–60% of normal levels of enzymatic activity in CNS are indicated in devastating diseases model and possibly to some disease-specific factors [10]. One of the possible explanations for the insufficient GALC activity in spinal cords of AAV2/5-treated twitcher mice might be due to insufficient titers or dosages of vectors for dispersal of the transgene throughout the neuraxis. To improve efficacy, a higher viral titer or repeated administrations of therapeutic vectors may be able to further increase transduction in the spinal cord [40]. Alternatively, molecular engineering of the capsid of the AAV vector offers promise for high-efficiency transduction at lower doses of injection vector [41]. Another possibility for the insufficient transduction in the spinal cord may be due to the leakage of vector during intracranial injection, which is evidenced by strong GALC expression over the choroid plexus and peri-ependymal cells of lateral ventricles and fourth ventricles. The AAV vector was absorbed and sequestrated due to its appreciable transduction specificity to choroid plexus and peri-ependymal cells [42,43]. Using a vector that is able to gain entry and circulate within the subarachnoid space without being sequestrated by ependymal cells will allow for the dispersal of viruses into multiple locations. Alternatively, an approach with intrathecal or cisterna magna

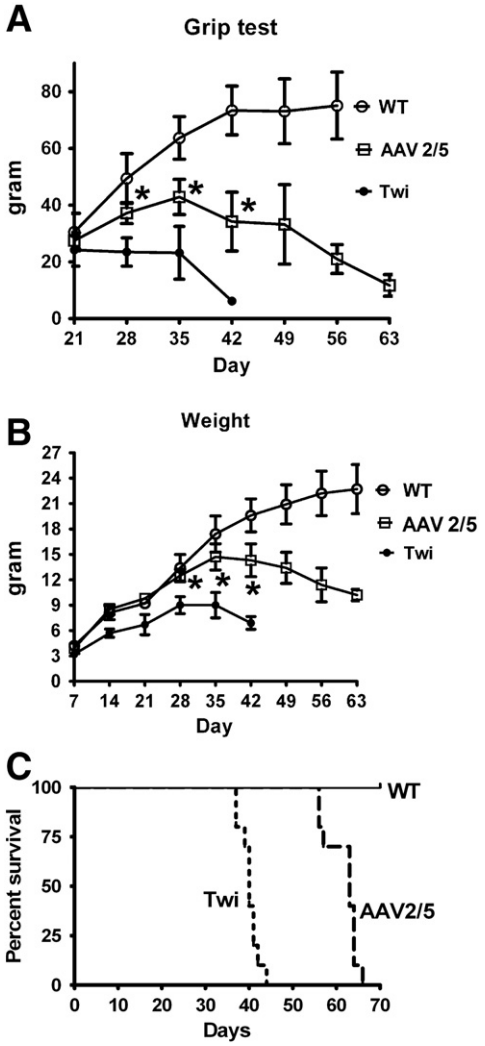

Fig. 6. Significant therapeutic benefit of AAV2/5 gene therapy on survival, weight loss, and motor dysfunction in twitcher mice. The neuromuscular strength by Grip test (A), and body weight (B) in untreated twitcher (Twi, n = 10), wild-type mice (WT, n = 10), and AAV2/5-treatment group (AAV2/5, n = 15) was measured weekly until death. (C) Kaplan–Meier analysis of survival curve for wild-type (WT, n = 10), untreated twitcher (Twi, n = 10), and AAV2/5-treated twitcher (AAV2/5, n = 15) mice. The asterisk indicates a significant difference from untreated twitcher mice. * Indicates significance of $p<0.05$ between AAV2/5-treated twitcher mice and untreated twitcher mice.

administration of viral vectors may distribute vectors more globally in the CNS; however, this approach may not supply enough enzymes to correct the entire brain due to the limitation of transduced cells located mainly in the CNS epithelia structures.

4.6. Efficacy of CNS-targeted gene therapy

By a cohort comparison using Kaplan–Meier analysis, the intracerebral-and-intracerebellar AAV2/5 delivery regimen used in this study provided significantly better therapeutic performance than our pilot intracerebral injection of AAV2/5-GALC in the twitcher mice [9]. It should be noted that the difference between these previously treated mice and the present work is the administration of the therapeutic vector to the cerebellum instead of the thalamus. The efficacy of intracerebral-and-intracerebellar injection of therapeutic vector was also observed in LINCL mice, which showed preservation of Purkinje cells, prevention of axonal degeneration and storage accumulation, preserved motor function and prolonged lifespan [44]. Both of our report and previous studies further highlighted the crucial role of targeting both cerebrum and cerebellum for distributing vector globally in CNS in designing intervention for LSD with cerebellum involvement [24,44].

4.7. Limitations of this study

Although our treatment was efficacious in treating the pathological, functional, and survival phenotypes of a severe mouse model of GLD, these treated animals eventually showed compromised motor impairment. In an analysis of immunohistopathology, the spinal cords of treated twitcher mice still showed remarkable demyelination and astrogliosis comparable to those of untreated twitcher mice. These findings implied the interruption of neuronal circuits between brain and spinal cord, which leads to the motor deterioration in those treated twitcher mice. Similar motor dysfunction was also evident in ablation of the cerebellar peduncles and corticospinal tract in murine models [45]. In this study, the interruption of neuronal circuits may arise from the failure in clearing psychosine in spinal cords due to the insufficient correction of GALC activity (6%). The inability to clear psychosine causes pathologic changes in oligodendrocytes and Schwann cells, possibly by disrupting membrane microdomains and some of the associated downstream signaling events [46,47], and leads to excessive demyelination and axonal degeneration in the twitcher mice. Interestingly, the regions of brain with robust expression of GALC activity showed significant reduction of psychosine levels and prevention of demyelination and axonopathy. These findings are in agreement with previous reports, suggesting that psychosine levels in CNS were reduced only when significant GALC activity was reached [12]. Furthermore, the inability to completely clear the accumulation of psychosine by supraphysiological levels of GALC indicated that there are additional aspects of the disease that dictate progression are not reversed by GALC gene augmentation. Combing cell therapy such as bone marrow transplantation with treatment aimed to reduction of inflammation and replacing dead or dying oligodendrocytes may provide a synergistic and more complete correction of this disease [11,12].

5. Conclusion

In conclusion, the information in this study validates the efficacy of this gene delivery approach to correct enzymatic deficiency, psychosine accumulation and neuropathy in CNS of GLD. A more robust response in the spinal cord, combined with a treatment able to target the PNS, would be desirable.

Disclosure/conflict of interest

There are no conflicts of interest to disclose.

Acknowledgments

We would like to acknowledge the efforts of Dr. P.H. Tu, M.D., Ph.D., for his critical review of the manuscript. We also thank S.R. Kaufman for his critical reading of the manuscript. This work was supported by the National Science Council [NSC-95-2745, NSC-99-2413] and grants from the Mackay Memorial Hospital [MMH9803, MMH9928, MMH-CT9904 and MMH-CY9905].

References

[1] K. Suzuki, Y. Suzuki, Globoid cell leucodystrophy (Krabbe's disease): deficiency of galactocerebroside beta-galactosidase, Proc. Natl. Acad. Sci. U.S.A. 66 (1970) 302–309.
[2] D.A. Wenger, M.A. Rafi, P. Luzi, Molecular genetics of Krabbe disease (globoid cell leukodystrophy): diagnostic and clinical implications, Hum. Mutat. 10 (1997) 268–279.
[3] K. Suzuki, M. Taniike, Murine model of genetic demyelinating disease: the twitcher mouse, Microsc. Res. Technol. 32 (1995) 204–214.

[4] K. Suzuki, P.M. Hoogerbrugge, B.J. Poorthuis, D.W. Bekkum, The twitcher mouse. Central nervous system pathology after bone marrow transplantation, Lab. Invest. 58 (1988) 302–309.
[5] P.K. Duffner, V.S. Caviness Jr., R.W. Erbe, M.C. Patterson, K.R. Schultz, D.A. Wenger, C. Whitley, The long-term outcomes of presymptomatic infants transplanted for Krabbe disease: report of the workshop held on July 11 and 12, 2008, Holiday Valley, New York, Genet. Med. 11 (2009) 450–454.
[6] M.S. Sands, B.L. Davidson, Gene therapy for lysosomal storage diseases, Mol. Ther. 13 (2006) 839–849.
[7] J.S. Shen, K. Watabe, T. Ohashi, Y. Eto, Intraventricular administration of recombinant adenovirus to neonatal twitcher mouse leads to clinicopathological improvements, Gene Ther. 8 (2001) 1081–1087.
[8] M.A. Rafi, H. Zhi Rao, M.A. Passini, M. Curtis, M.T. Vanier, M. Zaka, P. Luzi, J.H. Wolfe, D.A. Wenger, AAV-mediated expression of galactocerebrosidase in brain results in attenuated symptoms and extended life span in murine models of globoid cell leukodystrophy, Mol. Ther. 11 (2005) 734–744.
[9] D. Lin, C.R. Fantz, B. Levy, M.A. Rafi, C. Vogler, D.A. Wenger, M.S. Sands, AAV2/5 vector expressing galactocerebrosidase ameliorates CNS disease in the murine model of globoid-cell leukodystrophy more efficiently than AAV2, Mol. Ther. 12 (2005) 422–430.
[10] A. Lattanzi, M. Neri, C. Maderna, I. di Girolamo, S. Martino, A. Orlacchio, M. Amendola, L. Naldini, A. Gritti, Widespread enzymatic correction of CNS tissues by a single intracerebral injection of therapeutic lentiviral vector in leukodystrophy mouse models, Hum. Mol. Genet. 19 (2010) 2208–2227.
[11] D. Lin, A. Donsante, S. Macauley, B. Levy, C. Vogler, M.S. Sands, Central nervous system-directed AAV2/5-mediated gene therapy synergizes with bone marrow transplantation in the murine model of globoid-cell leukodystrophy, Mol. Ther. 15 (2007) 44–52.
[12] F. Galbiati, M.I. Givogri, L. Cantuti, A.L. Rosas, H. Cao, R. van Breemen, E.R. Bongarzone, Combined hematopoietic and lentiviral gene-transfer therapies in newborn Twitcher mice reveal contemporaneous neurodegeneration and demyelination in Krabbe disease, J. Neurosci. Res. 87 (2009) 1748–1759.
[13] N. Sakai, K. Inui, N. Tatsumi, H. Fukushima, T. Nishigaki, M. Taniike, J. Nishimoto, H. Tsukamoto, I. Yanagihara, K. Ozono, S. Okada, Molecular cloning and expression of cDNA for murine galactocerebrosidase and mutation analysis of the twitcher mouse, a model of Krabbe's disease, J. Neurochem. 66 (1996) 1118–1124.
[14] D.A. Wenger, C. Williams, Screening for lysosomal disorders, in: F.A. Hommes (Ed.), Techniques in Diagnostics Human Biochemical Genetics, Wiley-Liss, New York, 1991, pp. 587–617.
[15] W.C. Lee, A. Courtenay, F.J. Troendle, M.L. Stallings-Mann, C.A. Dickey, M.W. DeLucia, D.W. Dickson, C.B. Eckman, Enzyme replacement therapy results in substantial improvements in early clinical phenotype in a mouse model of globoid cell leukodystrophy, FASEB J. 19 (2005) 1549–1551.
[16] D. Dolcetta, L. Perani, M.I. Givogri, F. Galbiati, A. Orlacchio, S. Martino, M.G. Roncarolo, E. Bongarzone, Analysis of galactocerebrosidase activity in the mouse brain by a new histological staining method, J. Neurosci. Res. 77 (2004) 462–464.
[17] H. Ida, O.M. Rennert, K. Watabe, Y. Eto, K. Maekawa, Pathological and biochemical studies of fetal Krabbe disease, Brain Dev. 16 (1994) 480–484.
[18] S.M. LeVine, D.L. Wetzel, A.J. Eilert, Neuropathology of twitcher mice: examination by histochemistry, immunohistochemistry, lectin histochemistry and Fourier transform infrared microspectroscopy, Int. J. Dev. Neurosci. 12 (1994) 275–288.
[19] M. Taniike, K. Suzuki, Spacio-temporal progression of demyelination in twitcher mouse: with clinico-pathological correlation, Acta Neuropathol. 88 (1994) 228–236.
[20] K. Mikoshiba, M. Fujishiro, S. Kohsaka, H. Okano, K. Takamatsu, Y. Tsukada, Disorders in myelination in the twitcher mutant: immunohistochemical and biochemical studies, Neurochem. Res. 10 (1985) 1129–1141.
[21] M. Griffey, S.L. Macauley, J.M. Ogilvie, M.S. Sands, AAV2-mediated ocular gene therapy for infantile neuronal ceroid lipofuscinosis, Mol. Ther. 12 (2005) 413–421.
[22] C.N. Cearley, J.H. Wolfe, A single injection of an adeno-associated virus vector into nuclei with divergent connections results in widespread vector distribution in the brain and global correction of a neurogenetic disease, J. Neurosci. 27 (2007) 9928–9940.
[23] J.C. Dodge, J. Clarke, A. Song, J. Bu, W. Yang, T.V. Taksir, D. Griffiths, M.A. Zhao, E.H. Schuchman, S.H. Cheng, C.R. O'Riordan, L.S. Shihabuddin, M.A. Passini, G.R. Stewart, Gene transfer of human acid sphingomyelinase corrects neuropathology and motor deficits in a mouse model of Niemann–Pick type A disease, Proc. Natl. Acad. Sci. U.S.A. 102 (2005) 17822–17827.
[24] M.A. Passini, J.C. Dodge, J. Bu, W. Yang, Q. Zhao, D. Sondhi, N.R. Hackett, S.M. Kaminsky, Q. Mao, L.S. Shihabuddin, S.H. Cheng, D.E. Sleat, G.R. Stewart, B.L. Davidson, P. Lobel, R.G. Crystal, Intracranial delivery of CLN2 reduces brain pathology in a mouse model of classical late infantile neuronal ceroid lipofuscinosis, J. Neurosci. 26 (2006) 1334–1342.
[25] Y. Tanaka, H. Okado, T. Terashima, Retrograde infection of precerebellar nuclei neurons by injection of a recombinant adenovirus into the cerebellar cortex of normal and reeler mice, Arch. Histol. Cytol. 70 (2007) 51–62.
[26] M.L. Broekman, L.A. Tierney, C. Benn, P. Chawla, J.H. Cha, M. Sena-Esteves, Mechanisms of distribution of mouse beta-galactosidase in the adult GM1-gangliosidosis brain, Gene Ther. 16 (2009) 303–308.
[27] B.K. Berges, S. Yellayi, B.A. Karolewski, R.R. Miselis, J.H. Wolfe, N.W. Fraser, Widespread correction of lysosomal storage in the mucopolysaccharidosis type VII mouse brain with a herpes simplex virus type 1 vector expressing beta-glucuronidase, Mol. Ther. 13 (2006) 859–869.
[28] S. Giannetti, M. Molinari, Cerebellar input to the posterior parietal cortex in the rat, Brain Res. Bull. 58 (2002) 481–489.
[29] T.J. Ruigrok, A. Pijpers, E. Goedknegt-Sabel, P. Coulon, Multiple cerebellar zones are involved in the control of individual muscles: a retrograde transneuronal tracing study with rabies virus in the rat, Eur. J. Neurosci. 28 (2008) 181–200.
[30] D. Sondhi, D.A. Peterson, A.M. Edelstein, K. del Fierro, N.R. Hackett, R.G. Crystal, Survival advantage of neonatal CNS gene transfer for late infantile neuronal ceroid lipofuscinosis, Exp. Neurol. 213 (2008) 18–27.
[31] M.A. Passini, J.H. Wolfe, Widespread gene delivery and structure-specific patterns of expression in the brain after intraventricular injections of neonatal mice with an adeno-associated virus vector, J. Virol. 75 (2001) 12382–12392.
[32] M.A. Passini, D.J. Watson, C.H. Vite, D.J. Landsburg, A.L. Feigenbaum, J.H. Wolfe, Intraventricular brain injection of adeno-associated virus type 1 (AAV1) in neonatal mice results in complementary patterns of neuronal transduction to AAV2 and total long-term correction of storage lesions in the brains of beta-glucuronidase-deficient mice, J. Virol. 77 (2003) 7034–7040.
[33] M.A. Colle, F. Piguet, L. Bertrand, S. Raoul, I. Bieche, L. Dubreil, D. Sloothaak, C. Bouquet, P. Moullier, P. Aubourg, Y. Cherel, N. Cartier, C. Sevin, Efficient intracerebral delivery of AAV5 vector encoding human ARSA in non-human primate, Hum. Mol. Genet. 19 (2010) 147–158.
[34] J.S. Bae, S. Furuya, Y. Shinoda, S. Endo, E.H. Schuchman, Y. Hirabayashi, H.K. Jin, Neurodegeneration augments the ability of bone marrow-derived mesenchymal stem cells to fuse with Purkinje neurons in Niemann–Pick type C mice, Hum. Gene Ther. 16 (2005) 1006–1011.
[35] T. Torashima, C. Koyama, A. Iizuka, K. Mitsumura, K. Takayama, S. Yanagi, M. Oue, H. Yamaguchi, H. Hirai, Lentivector-mediated rescue from cerebellar ataxia in a mouse model of spinocerebellar ataxia, EMBO Rep. 9 (2008) 393–399.
[36] C. Sevin, A. Benraiss, D. Van Dam, D. Bonnin, G. Nagels, L. Verot, I. Laurendeau, M. Vidaud, V. Gieselmann, M. Vanier, P.P. De Deyn, P. Aubourg, N. Cartier, Intracerebral adeno-associated virus-mediated gene transfer in rapidly progressive forms of metachromatic leukodystrophy, Hum. Mol. Genet. 15 (2006) 53–64.
[37] M. Strazza, A. Luddi, M. Carbone, M.A. Rafi, E. Costantino-Ceccarini, D.A. Wenger, Significant correction of pathology in brains of twitcher mice following injection of genetically modified mouse neural progenitor cells, Mol. Genet. Metab. 97 (2009) 27–34.
[38] A. Luddi, M. Volterrani, M. Strazza, A. Smorlesi, M.A. Rafi, J. Datto, D.A. Wenger, E. Costantino-Ceccarini, Retrovirus-mediated gene transfer and galactocerebrosidase uptake into twitcher glial cells results in appropriate localization and phenotype correction, Neurobiol. Dis. 8 (2001) 600–610.
[39] M. Jeyakumar, R.A. Dwek, T.D. Butters, F.M. Platt, Storage solutions: treating lysosomal disorders of the brain, Nat. Rev. Neurosci. 6 (2005) 713–725.
[40] M.B. Cachon-Gonzalez, S.Z. Wang, A. Lynch, R. Ziegler, S.H. Cheng, T.M. Cox, Effective gene therapy in an authentic model of Tay–Sachs-related diseases, Proc. Natl. Acad. Sci. U.S.A. 103 (2006) 10373–10378.
[41] L. Zhong, B. Li, C.S. Mah, L. Govindasamy, M. Agbandje-McKenna, M. Cooper, R.W. Herzog, I. Zolotukhin, K.H. Warrington Jr., K.A. Weigel-Van Aken, J.A. Hobbs, S. Zolotukhin, N. Muzyczka, A. Srivastava, Next generation of adeno-associated virus 2 vectors: point mutations in tyrosines lead to high-efficiency transduction at lower doses, Proc. Natl. Acad. Sci. U.S.A. 105 (2008) 7827–7832.
[42] B.L. Davidson, C.S. Stein, J.A. Heth, I. Martins, R.M. Kotin, T.A. Derksen, J. Zabner, A. Ghodsi, J.A. Chiorini, Recombinant adeno-associated virus type 2, 4, and 5 vectors: transduction of variant cell types and regions in the mammalian central nervous system, Proc. Natl. Acad. Sci. U.S.A. 97 (2000) 3428–3432.
[43] D.J. Watson, M.A. Passini, J.H. Wolfe, Transduction of the choroid plexus and ependyma in neonatal mouse brain by vesicular stomatitis virus glycoprotein-pseudotyped lentivirus and adeno-associated virus type 5 vectors, Hum. Gene Ther. 16 (2005) 49–56.
[44] M.A. Cabrera-Salazar, E.M. Roskelley, J. Bu, B.L. Hodges, N. Yew, J.C. Dodge, L.S. Shihabuddin, I. Sohar, D.E. Sleat, R.K. Scheule, B.L. Davidson, S.H. Cheng, P. Lobel, M.A. Passini, Timing of therapeutic intervention determines functional and survival outcomes in a mouse model of late infantile Batten disease, Mol. Ther. 15 (2007) 1782–1788.
[45] A. Gasbarri, A. Pompili, C. Pacitti, F. Cicirata, Comparative effects of lesions to the ponto-cerebellar and olivo-cerebellar pathways on motor and spatial learning in the rat, Neuroscience 116 (2003) 1131–1140.
[46] F. Galbiati, V. Basso, L. Cantuti, M.I. Givogri, A. Lopez-Rosas, N. Perez, C. Vasu, H. Cao, R. van Breemen, A. Mondino, E.R. Bongarzone, Autonomic denervation of lymphoid organs leads to epigenetic immune atrophy in a mouse model of Krabbe disease, J. Neurosci. 27 (2007) 13730–13738.
[47] A.B. White, M.I. Givogri, A. Lopez-Rosas, H. Cao, R. van Breemen, G. Thinakaran, E.R. Bongarzone, Psychosine accumulates in membrane microdomains in the brain of krabbe patients, disrupting the raft architecture, J. Neurosci. 29 (2009) 6068–6077.